Magnetofluidic concentration and separation of non-magnetic particles using two magnet arrays

Magnetofluidic concentration and separation of non-magnetic particles using two magnet arrays

Majid Hejazian[a], Nam-Trung Nguyen[a]

Queensland Micro and Nanotechnology Centre, Griffith University, Brisbane, QLD 4111, Australia

E-mail: nam-trung.nguyen@griffith.edu.au;

Fax: +61 07 373 58021; Tel: +61 07 373 53921

The present paper reports the use of diluted ferrofluid and two arrays of permanent magnets for the size-selective concentration of non-magnetic particles. The micro magnetofluidic device consists of a straight channels sandwiched between two arrays of permanent magnets. The permanent magnets create multiple capture zones with minimum magnetic field strength along the channel. The complex interaction between magnetic forces and hydrodynamic force allows the device to operate in different regimes suitable for concentration of non-magnetic particles with small difference in size. Our experimental results show that non-magnetic particles with diameters of 3.1 μm and 4.8 μm can be discriminated and separated with this method. The results from this study could be used as a guide for the design of size-sensitive separation devices for particle and cell based on negative magnetophoresis.

I. INTRODUCTION:

Magnetofluidics is a research area that utilises the phenomena caused by magnetism and fluid flow leading to novel applications in the microscale.[1] External magnetic field has been widely used for continuous separation of cells and particles based on their size or magnetic susceptibility. The capability of contactless manipulation of species inside a microchannel is the remarkable advantage of micro magnetofluidics – the combination of magnetism and microfluidics.[2, 3] Pamme systematically reviewed the exploitation of magnetic force in the field of microfluidics including various functions such as trapping, transport, separation, and mixing.[4] Sorting of cells and particles using magnetofluidics could be achieved by trapping, focusing or deflection. A variety of methods have been reported in the literature on the separation by deflection and concentration by trapping of cells and particles, taking advantage of magnetic force.

Separation and sorting of cells and particles by deflection has been explored extensively. There are two basic concepts for separation of particles and cells using magnetic field: positive and negative magnetophoresis. Positive magnetophoresis is the migration of particles with a magnetic suseptibilitiy higher than that of the surrounding fluid. With positive magnetophoresis, the particles are attracted towards regions with higher magnetic field strength. On the other hand, negative magnetophoresis occurs when magnetic susceptibility of

the surrounding fluid is higher than that of the particles. With negative magnetophoresis, the particles move to regions with lower magnetic field strength.

Pamme and Wilhelm reported the use of positive magnetophoresis for continuous sorting of mouse macrophages and human ovarian cancer cells (HeLa cells).[5] Magnetic nanoparticles were used to label the cells. The extent of deflection and consequently the effectiveness of separation depend on the size of the cells and the flow rate. Khashan et al. applied computational fluid dynamics (CFD) to simulate the positive magnetophoretic separation of magnetically labelled cells in a microchannel.[6] Chung et al. used the so-called magnetic tweezers to separate magnetic microparticles with positive magnetophoresis technique in a microfluidic device.[7] At a relatively low flow rate, the method can achieve a separation rate as high as 81%. Combining with optical tweezers, magnetic tweezers may yield an even higher separation rate for a broader range of flow rate. Lateral separation of superparamagnetic beads and labelled breast adenocarcinoma MCF-7 cells, utilizing positive magnetophoresis were achieved using an angled permanent magnet.[8] A numerical model was formulated to predict the separation phenomenon. Liang et al. employed dilute ferrofluid as the carrier fluid in order to simultaneously use positive and negative magnetophoresis to further improve the separation of magnetic and non-magnetic particles.[9] An analytical model was employed to predict the deflection of particles in both ferrofluid and water.

Gelszinnis et al. reported a magnetic composite material, i-PDMS, to capture and separate paramagnetic beads with positive magnetophoresis technique.[10] The composite generates high local magnetic field gradients when placed between two permanent magnets. The effects of the resolution of the microstructures and the flow rate on the trapping and deflection of the particles were investigated. Zhu et al. employed ferrofluid to separate a mixture of particles with different magnetic properties using a combination of positive and negative magnetophoresis.[11] This separation method is label-free and relies only on intrinsic properties of the cells or particles. Kim and Kim numerically investigated the positive magnetophoretic separation of malaria-infected red blood cells from whole blood.[12] Malaria-infected was considered as paramagnetic particles suspended in a Newtonian fluid in their model. The design parameters such as magnetic pole array pitch, channel height, channel length and the flow rate were optimized to achieve the maximum capturing efficiency. Recently, Wu et al. numerically modelled positive magnetophoretic separation of malaria-infected red blood cells (RBCs) in a two-dimensional parallel-plate system using Eulerian–Lagrangian approach.[13] The blood plasma was considered as a Newtonian fluid, while the RBCs were modelled as soft paramagnetic spheres affected by drag and magnetic force, as well as their collisions. Using a constriction of 50-μm high and a 2-mm long diffuser could

improve the overall separation efficiency. Zhang et al. designed a microfluidic device using 3D printing technology.[14] Efficient and rapid extraction of spiked Human Papillomavirus (HPV) 18 plasmids was achieved. In addition, a kinetics model was developed for adsorption of nucleic acids on cellulose functionalized superparamagnetic beads using positive magnetophoresis. Scherr et al. investigated protein capture using positive magnetophoresis and compared the performance of one and two magnets configurations.[15] The two-magnet configuration demonstrated a higher efficiency and more rapid extraction of target biomarkers compared to the one magnet system. Wang et al. developed an automated and low-cost PMMA-tape-glass microfluidic system.[16] The device prepares single-stranded DNA for magnetic bead-based microarray analysis using two on-chip mixing valves, a magnet for the manipulation of magnetic beads with positive magnetophoresis.

Magnetic levitation can enable label-free separation and monitoring of different cell populations based on their magnetic and density signatures. Knowlton et al. used a pair of magnets with the same poles facing each other aligns the magnetic field with the gravitational field, allowing diamagnetic particles or cells suspended in a paramagnetic fluid to be focused and separated.[17] Calibrating the levitation heights may estimate the densities of the particles precisely. Furthermore, the authors used a smartphone platform for label-free and sensitive detection sickle cells. The separation concept takes advantage of the higher density of sickle red blood cells under deoxygenated conditions.[18] Tasoglu et al. reported label-free separation and monitoring of different cell types utilizing magnetic levitation.[19] The system utilizes a pair of magnets with same poles facing each other to focus the cells. Circulating cancer cells, sickled RBCs, and healthy RBCs suspended in gadolinium-based paramagnetic medium were tested. Rapid spatial separation of the different cell populations was achieved.

Trapping and concentrating of cells and particles has potential applications in chemical and biological studies. Ahn et al. reported one of the earliest microfluidic devices for the manipulation of magnetic particles in a dilute suspension.[20] Integrated electromagnets induce a magnetic field that traps magnetic particles in the flow without physical barriers. The trapped particles were released after removing the magnetic field by turning off the electromagnet. Winkleman et al. reported a three-dimensional magnetic trap for non-magnetic particles such as living cells in a paramagnetic solution.[21] The concentration of paramagnetic salt was maintained at a low level to keep the cells viable. Because of the relatively low field strength, field gradient and susceptibility mismatch, the device can only trap particles larger than 5 μm in diameter. Ramadan and Gijs reported a continuous-flow microfluidic device with rotating magnetic field for trapping and releasing of magnetic particles.[22] The rotating permanent magnets periodically arranged the magnetic field for periodic trapping and

releasing of particles, allowing continuous concentrating, washing and purifying of magnetic particles in the device.

Teste et al. reported a lab-on-a-chip device with a magnetic chamber packed with ferromagnetic iron beads to trap 30-nm magnetic nanoparticles.[23] The iron beads increase the local magnetic field gradient and thus improve the trapping efficiency of the magnetic nanoparticles. Watarai and Namba investigated the impact of a non-uniform magnetic field on non-magnetic micro particles suspended in a paramagnetic manganese(II) chloride solution[24]. They observed that when the particles approach the pair of magnets, the direction and the magnitude of their velocity change significantly. The magnetophoretic buoyancy exerted on the particles creates a magnetophorectic velocity and leads to capture of particles in the area with minimum magnetic field. In another work[25] the authors reported a improved performance with a pair of small iron tips attached to the Nd–Fe–B magnets. The magnetophoretic velocity of 3-μm polystyrene microparticles in 0.6 M manganese(II) chloride solution was determined. Furthermore, the authors investigated the magnetophoresis of a single human blood cell in 0.1 M manganese(II) solution and estimated its magnetic susceptibility.

Aki et al. developed a microelectromagnetic system with a non-uniform magnetic field to trap nonmagnetic microparticles and yeast.[26] Polystyrene particles and yeast cells were trapped at regions with non-uniform magnetic field. Bucak et al. developed a continuous counter current separation system based on magnetophoresis principle.[27] The non-magnetic microparticles experience a magnetophoretic force in the direction of decreasing magnetic field strength. The device could successfully concentrate and separate non-magnetic microparticles suspended in ferrofluid under a nonuniform magnetic field. Zeng et al. demonstrated the concentration of polystyrene particles and live yeast cells from a ferrofluid solution using negative magnetophoresis.[28] A pair of attracting magnets creates a non-uniform field. Peyman et al. studied the possible applications that could be achieved based on negative magnetophoresis.[29] Trapping, focussing and deflection of polystyrene particles were demonstrated by changing the arrangement of magnets along the microfluidic device. Zhou et al. examined simultaneous trapping of diamagnetic and magnetic particles in different locations of a microfluidic device.[30] A T-shaped microfluidic device with a single permanent magnet was used to concentrate both particles from a ferrofluid flow. Tarn et al. reported simultaneous trapping of magnetic and non-magnetic particles with a pair of permanent magnets.[31] In an aqueous solution of manganese (ii) chloride, magnetic particles were trapped between the magnets, while non-magnetic particles were trapped outside this zone. Eisentrager et al. reported a model of a periodic array of magnetised cylinders for high-gradient magnetic separation of particles.[32]

We previously demonstrated the effect of bulk magnetic force on diluted ferrofluids.[33, 34] We showed experimentally that a body force caused by susceptibility mismatch and magnetic field gradient can compete with the hydrodynamic drag force of the flow and the negative-magnetophoretic force in the transport process of suspended non-magnetic particles. The present work systematically studies the relative roles of these forces to identify the dominating force in a wide range of operation conditions. The dominance of each force leads to a trapping regime that potentially leads to the separation and concentration applications. For this purpose, a magnetofluidic device was fabricated. Two arrays of attracting magnets are placed next to the straight microchannel. The device was tested for a range of ferrofluid concentrations and flow rates to assess the competition between the magnetically induced phenomena and hydrodynamic drag. Our device was able to separate non-magnetic polystyrene (PS) particles with a size difference of only 1.6 μm. Required susceptibility mismatch could be created by adjusting the concentration of the diluted ferrofluid for different purposes for different sizes of the particle. Furthermore, the results from this study could be applied in designing a separation system based on deflection, since we report the effect of balance between dominant forces on particle manipulation. Considering the fact that the device works based on the negative magnetophoresis effect, trapping of both magnetic and non-magnetic particles is possible. The experimental results form an operation map to guide future research in this area and could lead to a variety of applications such as cell separation, concentration and sample preparation.

II. MATERIALS AND METHODS

Figure 1 shows the schematic of the channel and the magnet arrays used in our experiments. The straight channel has a width of W=1 mm, a height of H=500 μm. We used a laser engraving machine (Trotec/Rayjet) to cut the channel through a clear 500-μm thick double-sided adhesive tape. The channel was then sandwiched between a glass slide and a poly(methyl methacrylate) PMMA slide. The slots for the magnets were cut through the PMMA slide before bonding to the tape. Neodymium–iron–boron (NdFeB) permanents magnet cubes with a volume of 3.2 mm^3, and grade of N42 (B222, K&J Magnetics Inc.) were placed in two arrays on both sides of the channel, with 11 magnets on each side. The magnetic field magnitude of the individual permanent magnet versus distance from the magnet was measured and reported previously.[34] A precision syringe pump (SPM100, SIMTech Microfluidics Foundry) delivers the fluid into the channel. The flow rate in the later experiments ranges from 1 to 400 μL/min. A charge-coupled device (CCD) camera (Edmund Optics, Germany) attached to an inverted microscope (Nikon Eclipse TE100) and connected to a desktop computer was used for visualization

and image recording. Diluted water-based ferrofluid (EMG707, Ferrotec) was used as the paramagnetic liquid in the experiments. The commercial ferrofluid has an initial magnetic susceptibility of 0.12, a magnetic particle concentration of 2 % vol., and a saturation magnetization of 110 Gauss. The ferrofluid was further diluted by DI water into eight different concentrations: 0.25, 0.5, 0.75, 1, 2, 5, 20, and 50%vol. Fluorescent polystyrene (PS) particles (ThermoScientific Inc.) with different sizes and colours (3.1 μm, red) and (4.8 μm, green) were suspended in the diluted ferrofluid samples.

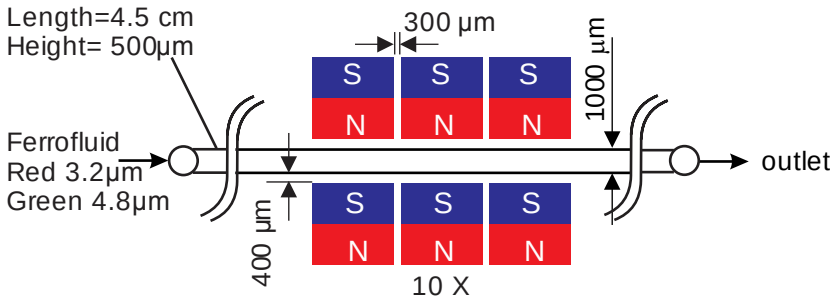

FIG.1 Schematic of the channel and the magnet arrays.

III. THEORETICAL BACKGROUND

Three dominant forces are involved in manipulating non-magnetic particles in a paramagnetic liquid: negative magnetophoretic force caused by the magnetic field on the particles which moves the particles towards magnetic field minimum, hydrodynamic drag force caused by the fluid flow and in the direction of the flow, and magnetoconvective drag force. Magnetoconvective flow is the result of a bulk force induced by the magnetic field on a paramagnetic fluid, in the direction of magnetic field maximum. The competition between these forces determines whether the particles could be trapped at a given position or transported along a particular trajectory. The magnetic energy of a spherical magnetic particle exposed to a magnetic field is estimated as:[1]

$$E_m = \frac{\pi}{6} d^3 MB \qquad (1)$$

where E_m is the magnetic energy, M is the magnetization of the particle, d is the diameter of the particle, B is the magnetic flux density. For suspended particles in a flow, frictional energy can be estimated as:

$$E_f = 3\pi\eta d^2 u \qquad (2)$$

where E_f is the frictional energy, and u is the velocity. We use the ratio between magnetic and frictional energies to evaluate the stability of the particles. For this purpose, the dimensionless characteristic number is magnetophoretic stability number:

$$S_{mp} = \frac{E_m}{E_f} = \frac{1}{18}\frac{MBd}{\eta u} \qquad (3)$$

According to equation (3), the magnetophoretic stability number is a function of microparticles diameter, magnetic susceptibility and viscosity of the ferrofluid. The value of magnetophoretic stability number is highly affected by ferrofluid concentration and flow rate. On the other hand, the intensity of magnetic field varies with distance from the magnets. Evaluating this number at capture zones and relating the values to the experimental data lead to an operation map, which can provide the required values of concentration and flow rate to achieve particle capture.

We used COMSOL (COMSOL Inc., USA) to simulate the distribution of magnetic flux density created by the magnet array. Magnetic insulation is considered around the whole system. Figure 2(a) shows the typical simulated magnetic field in the microchannel between a pair of magnets. The simulation was carried out with water inside the channel, only to illustrate the distribution of the magnetic field. The simulation result indicates that the actual field maxima are located outside the channel, between the edges of the magnets. Within the channel, periodic traps of field maxima and minima are at the channel walls facing the magnets and between the magnet poles, respectively. The trapping behaviour in these locations will be investigated in details.

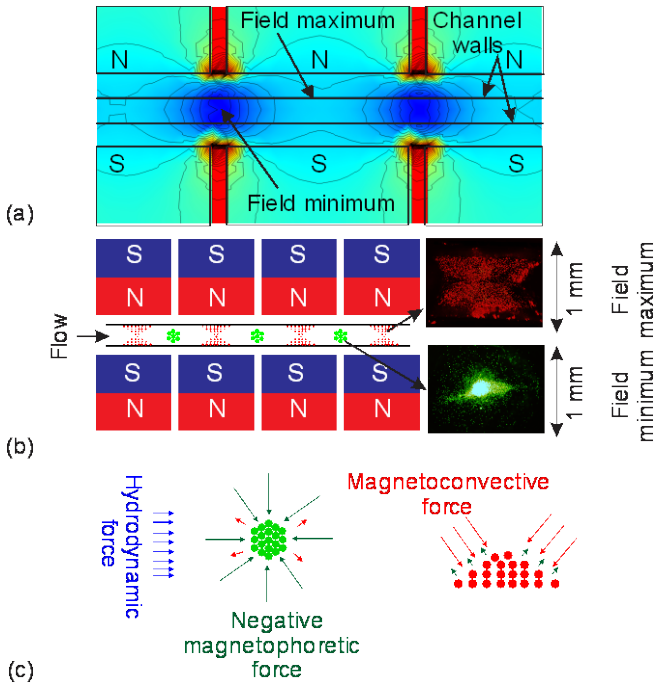

FIG. 2 The concept of micro magnetofluidic concentration: (a) The simulated magnetic field. The dark blue areas (colour online) are the minimum magnetic field traps created in between the attracting magnet pairs. (b) Schematic of the size-selective traps for non-magnetic particles, green dots represent large particles, red dots represent small particles (flow rate of 10 μL/min, volume concentration of 1%). (c) Schematic description of dominant forces and their direction.

IV. RESULTS AND DISCUSSION

Ferrofluid samples with various concentrations from very diluted to highly concentrated content of magnetic nanoparticles were prepared. Two sizes of fluorescent PS particles with different colours were suspended in all ferrofluid samples. Each sample was tested with a wide range of flow rates. The different concentrations lead to different susceptibilities, which in turn tune the magnitudes of magnetophoretic and negative magnetophoretic forces. Also by varying the flow rates, the magnitude of hydrodynamic forces can also be adjusted. The images from the experiment were taken after a few minutes, when the system reaches a steady state condition.

The trapping phenomenon and concentration modes

Two arrays of 11 magnets create 10 simultaneous spherical plugs of trapped non-magnetic particles along the channel. At a given flow rate and ferrofluid concentration, large particles are trapped in the gap between the two neighbouring magnets. The small non-magnetic particles accumulate on the wall next to the magnet poles, Fig. 2(b). Thus, size-selective concentration of non-magnetic particles can be achieved. Large non-magnetic particles are repelled from the regions with a higher magnetic field, because of the significant negative magnetophoresis force. Consequently, large particles cannot enter the region between two attracting magnets. The negative magnetophoretic force is large enough to trap them at locations with a minimum field strength and form spherical particle plugs along the channels.[25] The negative magnetophoretic fore is dominant for larger particles. The magnitude of the stability numbers is evaluated and presented later for each condition.

As mentioned above, large particles are captured at locations of field minima. Each particle plug forms an internal recirculation, which is created by the equilibrium between the negative magnetophoretic force acting on the particles, the magnetoconvective force on the ferrofluid and the hydrodynamic drag force of the main flow. Particles that escape the internal circulations of each plug feed the next one downstream. The escaped particles are focused into a line at the centre of the channel until they reach the next location of field minimum. Particles circulate around the minimum field zone, until they become almost stationary and trapped at its centre, Fig. 2(a).

This trapping pattern continues with the formation of the 10th circular trapping zone where the remaining particles exit the channel in a focused line. Meanwhile, small non-magnetic particles accumulate on the walls near the magnet poles, along with paramagnetic nanoparticles of the ferrofluid. These particles form a butterfly shape on each channel side with maximum field, Fig. 2(a). Escaped small particles bypass the trapping regions and feed into their next trap at the magnet poles.

As mentioned above, small red micro-particles are captured on the magnets poles, mixed with a pile of Iron oxide nanopartciles. Being in a close proximity of the magnet poles where strong magnetoconvective force exists, the small red particle plugs are not affected significantly by increasing flow rate. On the other hand, large green particles form clear circular capture zones and are very sensitive to the change of the flow rate. As a result, the green particle plugs are better representatives of the quality of particle capture and sorting in the system.

Effect of flow rate

We used a wide range of flow rates to observe the trapping behaviour with each ferrofluid concentration. An optimum flow rate exists for each concentration where a maximum number of particles were captured. At a given trapping zone and for a fixed concentration of 1% vol., a relatively low flow rate of 5 µL/min allows the large particles to slowly accumulate at the field minimum trap. The particle plug grows until it reaches a steady state condition and the diameter of the spherical plug becomes constant. This behaviour occurs as the result of the balance between negative magnetophoretic, magnetoconvective and hydrodynamic forces. Smaller particles accumulated as expected on the walls next to the magnet poles.

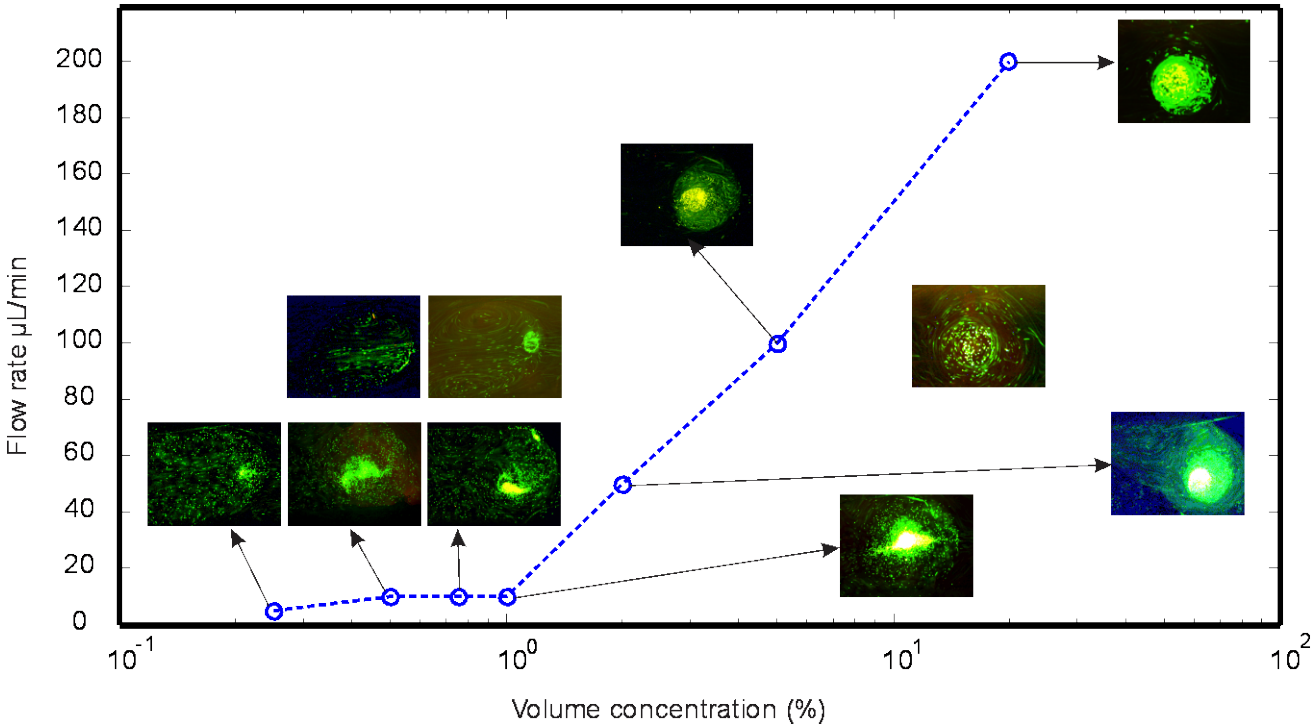

FIG. 3 The optimal flow rate for the different volume concentration of the commercial ferrofluid. The insets are images of 4.8-µm green particles at the first trapping zone from the channel inlet.

As the flow rate increases to 10 μL/min, we observe better trapping of the large particles. More particles are trapped as more particles are supplied with the higher flow rate. As a result, a larger particle plug is formed in the steady state condition.

As the flow rate increases significantly up to 50 and 100 μL/min, the number of captured particles reduces and the size of the plug becomes smaller. A large flow recirculation with two major vortexes next to the plug was observed at higher flow rates. Large particles cannot reach the force equilibrium, while fewer particles become stationary. Most particles escape the field-minimum trap and exit the channel, as the strong hydrodynamic force is dominant. This experiment indicates that there is an optimal flow rate for which the number of captured particles for size based concentration reaches its maximum. Figure 3 shows the relationship between the optimal flow rate and the ferrofluid concentration. The two particle types of our experiment could be separated with these optimal flow rates.

A. Effect of ferrofluid concentration

We prepared diluted ferrofluids with eight different concentrations ranging from 0.25% to 50 % vol. Figure 4 summarises the effect of concentration on particle trapping for three different flow rates. Three significant forces are involved in the trapping phenomenon: two drag forces and the negative magnetophoretic force. The drag forces are caused by the primary hydrodynamic flow and the secondary magnetoconvective flow, which is the magnetic body force exerted on the ferrofluid.[35] The balance between the three forces determines whether a particle with a given size could be separated and collected at the field minimum traps or at the field maximum traps. Furthermore, the balance between the forces can explain the shape and size of the trapping zones. Fig. 4 shows that very diluted ferrofluids such as 0.25 % vol. sample only forms particle plugs at lower flow rates. At higher flow rates, the negative magnetophoretic force is not strong enough to compete with hydrodynamic drag force to keep the particles stationary. At high flow rates, the resultant force keeps the particles moving in a circle at the trapping zone. Another interesting phenomenon observed with the lowest ferrofluid concentration is that both small and large particles are captured at the field minimum zones. Some large particles are even captured at the field maximum zones next to the magnet poles. However, the number of large particles trapped at the field maximum zones decreases significantly with increasing ferrofluid concentration.

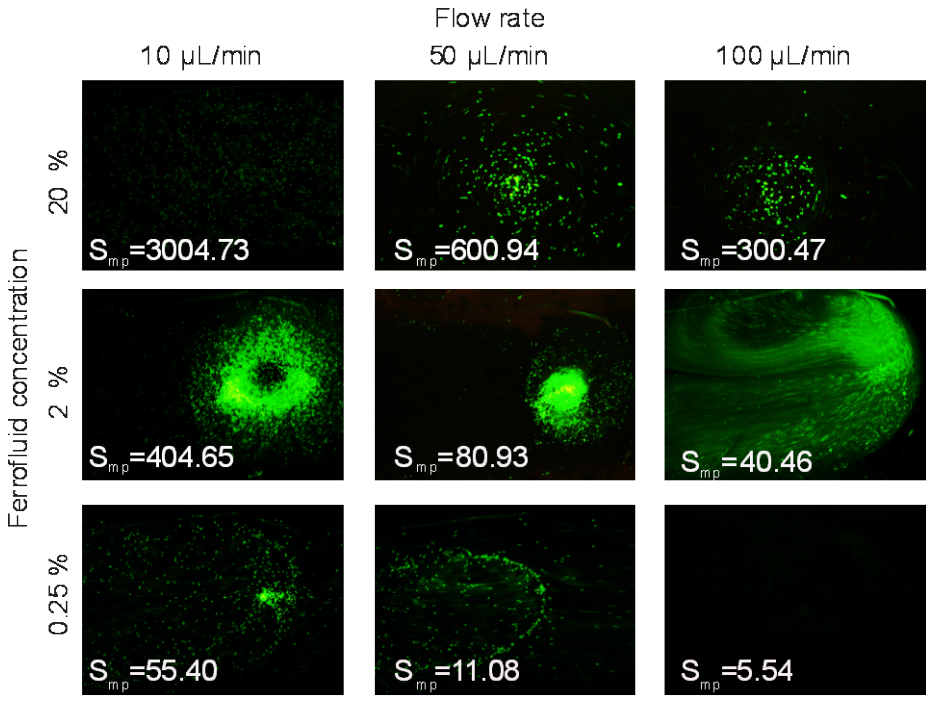

FIG. 4 The minimum field capture zones at different concentrations. Images show 4.8 µm fluorescent green particles captured.

The above observation proves that the concentration of ferrofluid should be high enough to yield a negative magnetophoretic force strong enough to trap large particles. Therefore, ferrofluid concentrations of less than 1 % vol. is not suitable for capturing 4.8-µm particles, while concentrations lower than 1 % vol. are appropriate for trapping the 3.2-µm particles.

The reason for large particles being trapped on the walls next to the magnet poles could be the magnetoconvective flow at the field maximum zone. A low ferrofluid concentration leads to a smaller magnetic susceptibility of the fluid and a weaker magnetoconvective force elsewhere in the flow. However, magnetic nanoparticles accumulate at the field maximum zones creating both high magnetic susceptibility and susceptibility gradient and consequently a strong local magnetoconvective secondary flow. The large particles are dragged by the flow and enter the regions with maximum magnetic field. The negative magnetophoretic force is weaker than the drag force caused by the local magnetoconvective flow preventing them from escaping the maximum-field zone. As result, some of the large particles are trapped at the field maximum zone. On the other hand, negative magnetophoretic force is dominant for small particles at low concentration allowing them to be trapped at field minimum zones.

At a concentration between 1% and 20 % vol., large particles are captured at the field minimum zones, while smaller particles are trapped at field maximum zones. Size-selective concentration can be achieved in this regime, as particles of different sizes were simultaneously captured at separate zones. The reason for trapping

small particles at field maximum zones with a high ferrofluid concentration is the dominant magnetoconvective secondary flow in these zones. Negative magnetophoretic force acting on large particles is dominant at field minimum zones. As the concentration reaches 50%, both particles are captured at field minimum zones at a rapid rate. The high magnetic susceptibility results in a powerful negative magnetophoretic force. Accumulation of particles at the field maximum zones was not observed.

Figure 4 shows another interesting phenomenon of the different shapes and sizes of trapping zones under the various sets of flow rate and ferrofluid concentration. The balance between magnetoconvective force and hydrodynamic force determines the size of the trapping zones. Magnetoconvective force expands the circular zone, while the hydrodynamic force compresses it. Consequently, a higher flow rate leads to a smaller zone. On the other hand, the hydrodynamic force also competes with the negative magnetophoretic force. Increasing flow rate leads to more particles circulating around the trapping zones and less stationary particles. Another noticeable phenomenon is the shape of a hollow plug under certain conditions. The empty region in the centre of the circular plugs is the result of the competition between magnetoconvective force that moves particles out of the zone, and negative magnetophoretic and hydrodynamic forces that push the particles into the centre of the trapping zone.

B. Trapping zones

As mentioned above, the magnet arrays create 10 field minimum zones along the channel of our device. In order to compare the different trapping zones, we fixed the ferrofluid concentration and the flow rate at 2% vol. and 20 μL/min, respectively. Figure 5 shows the images of the captured green 4.8-μm particles in the 10 zones along the channel. The flow is from right to left. The zones closer to the inlet can trap more particles. Further downstream, both magnetic nanoparticles of the ferrofluid and non-magnetic particles are depleted. Lower concentration of magnetic nanoparticles downstream lead to weaker magnetophoretic and magnetoconvective forces making the capture zone appears to be larger. Fewer non-magnetic particles makes the capture zone looks hollow.

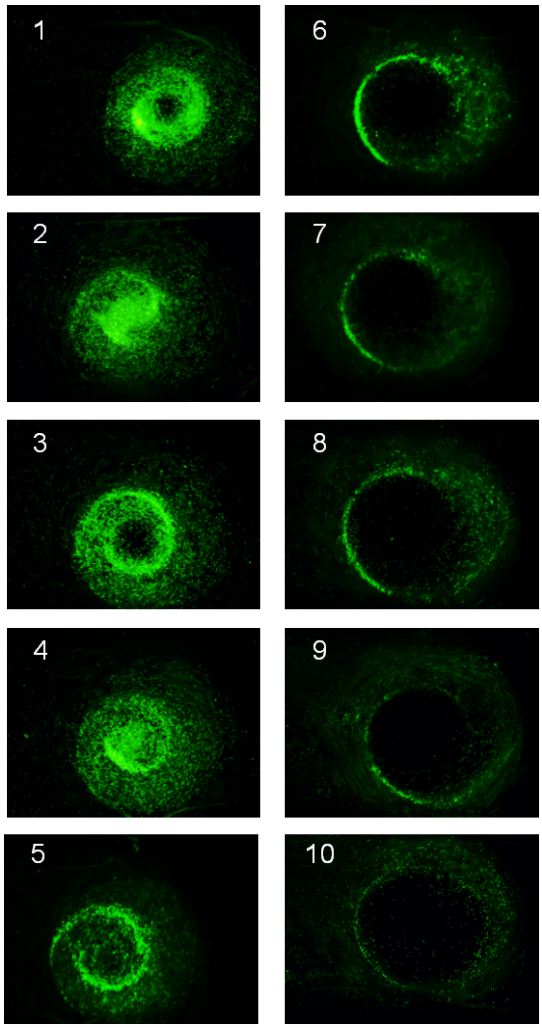

FIG. 5 All trapping zones (flow is from right to left, 1: close to the inlet, 10 close to the outlet) at 2 % vol. and 20 µL/min.

C. The operation map

We plot the different trapping and separation regimes on an operation map with the Reynolds number and the magnetophoretic stability number as the two dimensions of the space. The Reynolds number is the relative ratio between inertial force and friction force of the flow and represents the strength of the hydrodynamic force on the particles. The magnetophoretic stability number was defined in equation (3) as the ratio between magnetic and frictional energies representing the strength of magnetophoretic force. The present dimensions doe not include the magnetoconvetive effect.

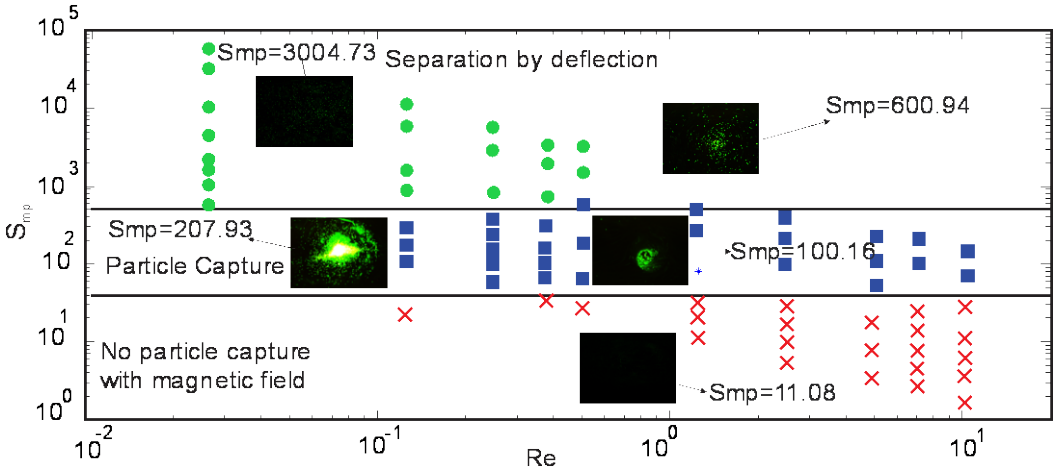

FIG. 6 Full operation map demonstrating the feasible separation methods in each range of S_{mp} and Re. (the points in the graph represent the experimental data that is available).

Figure 6 shows the S_{mp}-Re space as the operation map of our device. In our present work, trapping of both particle sizes happens in the range of $40<S_{mp}<400$. For $S_{mp}<40$ and $Re<1$, particles are not captured but circulate around the trapping zone. For $S_{mp}<40$ and $Re>1$, magnetic force no longer has any impact on the particles. Particle sorting by hydrodynamic force and inertial force is feasible in this region and the operation moves into the regime of inertial microfluidics. For $S_{mp}>400$ and $0.1<Re<10$, negative magnetophoretic and magnetoconvective forces are dominant. This region is suitable for size-selective concentration of particles. The size of non-magnetic particles should be considered to find the appropriate flow rate to achieve separation, as there is a competition between negative magnetophoretic and magnetoconvective force in this region. More diluted ferrofluids and lower flow rates are needed for the separation of small particles. A higher concentration of ferrofluids would trap small particles at field-maximum zones close to the magnet. On the other hand, more concentrated ferrofluid and a high flow rate are appropriate for separating large particles.

V. CONCLUSIONS

We designed, fabricated and characterised a magnetofluidic device for highly size-selective particle trapping and concentration. The device consists of two arrays of attracting magnets, which exert a non-uniform magnetic field on the ferrofluid flow inside the channel. We examined the effect of concentration and flow rate on the quality of particle trapping. Various concentrations of diluted ferrofluid were tested. The behaviour of the trapped particles is determined by three force types: negative magnetophoretic, magnetoconvective, and hydrodynamic forces. The impact of their competition was analysed and discussed. The balance between these forces determines the shape and size of the trapping zones, as well as the feasibility of particle separation. We used the magnetophoretic

stability number and Reynolds number to describe the effect of the force balance quantitatively. The magnitude of these numbers determines the regimes of size-selective separation by particle trapping, particle deflection or no separation. Furthermore, the operation map from this study can also be used to extend the study and predict the possibility of capture and sorting particles with different sizes. The key significance of the presented method is the capability of separating non-magnetic particles with a relatively high size-selectivity. The results presented here could be used as a guide for designing devices for separation of non-magnetic particles such as cells with small size difference using diluted ferrofluid.

ACKNOWLEDGMENTS

The authors acknowledge the funding support from Australian Research Council through linkage grant LP150100153.

REFERENCES

[1]N.-T. Nguyen, *Microfluid Nanofluid*. 12, 1-16 (2012).
[2]M. Hejazian, W. Lib and N.-T. Nguyen, *Lab Chip*. 15, 959–970 (2015).
[3]A. Lenshof and T. Laurell, *Chemical Society Reviews.* 39, 1203–1217 (2010).
[4]N. Pamme, *Lab Chip*. 6, 24–38 (2006).
[5]N. Pamme and C. Wilhelm, *Lab on a Chip*. 6, 974–980 (2006).
[6]S. A. Khashan, E. Elnajjar and Y. Haik, *Journal of Magnetism and Magnetic Materials. 323,* 2960–2967 (2011).
[7]Y.-C. Chung, P.-W. Chen, C.-M. Fu and J.-M. Wu, *Journal of Magnetism and Magnetic Materials.* 333, 87–92 (2013).
[8]T. P. Forbes and S. P. Forry, *Lab Chip.* 12, 1471–1479 (2012).
[9]L. Liang, C. Zhang and X. Xuan, *Appl. Phys. Lett.* 102, 234101-234104 (2013).
[10]R. Gelszinnis, M. Faivre, J. Degouttes, N. Terrier, R. Ferrigno and A.-L. Deman, *17th International Conference on Miniaturized Systems for Chemistry and Life Sciences 27-31 October 2013, Freiburg, Germany*.
[11]T. Zhu, R. Cheng, Y. Liu , J. He and L. Mao, *Microfluid Nanofluid*. 17, 973-982 (2014).
[12]J. Kim and C.-N. Kim, *Journal of Mechanical Science and Technology*. 29, 4833-4839 (2015).
[13]W. T. Wu, A. B. Martin, A. Gandini, N. Aubry, M. Massoudi and J. F. Antaki, *Microfluid Nanofluid*. 20-41, (2016).
[14]L. Zhang, R. N. Deraney and A. Tripathi, Biomicrofluidics 9, 064118 (2015).
[15]T. F. Scherr, H. B. Ryskoski, A. B. Doyle and F. R. Haselton, Biomicrofluidics 10, 024118 (2016).
[16]S. Wang, Y. Sun, W. Gan, Y. Liu, G. Xiang, D. Wang, L. Wang, J. Cheng and P. Liu, Biomicrofluidics 9, 024102 (2015).
[17]S. Knowlton, C. H. Yu, N. Jain, I. C. Ghiran, S. Tasoglu, PLOS ONE, 10, e0134400 (2015).
[18]S. M. Knowlton, I. Sencan, Y. Aytar, J. Khoory, M. M. Heeney, I. C. Ghiran, S. Tasoglu, Scientific Reports 5, 15022 (2015).
[19]S. Tasoglu , J. A. Khoory , H. C. Tekin , C. Thomas , A. E. Karnoub , I. C. Ghiran and U. Demirci, Adv. Mater. 27, 3901–3908 (2015).

[20]M. G. A. C. H. Ahn, W. Trimmer, Y. N. Jun and S. Erramilli, *J. Microelectromech. Syst.* 5, 151 (1996).
[21]C. P. Gooneratne, C. Liang, I. Giouroudi and J. Kosel, *Procedia Engineering* 25, 1201 – 1204 (2011).
[22]Q. Ramadan and M. A. M. Gijs, *Procedia Chemistry.* 1, 1499–1502 (2009).
[23]B. Teste, F. Malloggi, A.-L. Gassner, T. Georgelin, J.-M. Siaugue, A. Varenne, H. Girault and S. Descroix, *Lab Chip.* 11, 833 (2011).
[24]H. Watarai and M. Namba, *Analytical Sciences.* 17, 1233-1236 (2001).
[25]H. Watarai and M. Namba, *Journal of Chromatography A.* 961, 3–8 (2002).
[26]A. Aki, O. Ito, H. Morimoto, Y. Nagaoka, Y. Nakajima, T. Mizuki, T. Hanajiri, R. Usami and T. Maekawa, *JOURNAL OF APPLIED PHYSICS.* 104, 094509 (2008).
[27]S. Bucak, S. Sharpe, S. Kuhn and T. A. Hatton, *Biotechnol. Prog.* 27, 744-750 (2011).
[28]J. Zeng, C. Chen, P. Vedantam, T.-R. Tzeng and X. Xuan, *Microfluid Nanofluid.* 15, 49–55 (2013).
[29]S. A. Peyman, E. Y. Kwan, O. Margarson, A. Iles and N. Pamme, *Journal of Chromatography A.* 1216, 9055–9062 (2009).
[30]Y. Zhou, D. Thanjavur Kumar, X. Lu, A. Kale, J. DuBose, Y. Song, J. Wang, D. Li and X. Xuan, *Biomicrofluidics*. 9, 044102 (2015).
[31]M. D. Tarn, S. A. Peyman and N. Pamme, *RSC Adv.* 3, 7209–7214 (2013).
[32]A. Eisentrager, D. Vella and I. M. Griffiths, *Applied Physics Letters.* 105, 033508 (2014).
[33]G.-P. Zhu, M. Hejiazan, X. Huang and N.-T. Nguyen, *Lab Chip.* 14, 4609 (2014).
[34]M. Hejazian and N.-T. Nguyen, *Lab Chip.* 15, 2998–3005 (2015).
[35]T. Strek, *Finite Element Simulation of Heat Transfer in Ferrofluid*, INTECH Open Access Publisher, (2008).